3. O. M. Alifanov, Inzh.-Fiz. Zh., 29, No. 1, 13 (1975).
4. G. M. Kondrat'ev, Steady Thermal Conditions [in Russian], GITTL, Moscow (1954).
5. E. M. Berkovich, B. M. Budak, and A. A. Golubeva, in: Approximate Methods of Solving Problems of Optimal Control and Some Incorrect Inverse Problems [in Russian], MGU, Moscow (1972), p. 112.
6. E. M. Berkovich and A. A. Golubeva, in: The Solution of Problems of Optimal Control and Some Inverse Problems [in Russian], MGU, Moscow (1974), p. 59.
7. A. A. Samarskii, Introduction to the Theory of Difference Schemes [in Russian], Nauka, Moscow (1971).
8. E. M. Berkovich and A. A. Golubeva, The Solution of Problems of Optimal Control and Some Inverse Problems [in Russian], MGU, Moscow (1974), p. 100.
9. O. M. Alifanov, Inzh.-Fiz. Zh., 26, No. 4, 682 (1974).
10. E. M. Berkovich, A. A. Golubeva, et al., in: The Smelting and Casting of Nonferrous Metals and Alloys [in Russian], Part 47, Metallurgiya (Giprotsvetmetobrabotka), Moscow (1976), p. 80.

# IMPURITY DISTRIBUTION IN A MELT CRYSTALLIZING WITH CONVECTION CAUSED BY CONCENTRATION GRADIENTS

P. F. Zavgorodnii, V. I. Kolesnik, I. L. Povkh, and O. N. Lukicheva

UDC 532.72:669.015.23

Numerical calculations on a model show that concentration-dependent convection has a marked effect on the impurity distribution in the solid.

Chemical nonuniformity arises in the crystallization of a melt because of partition of impurities in the two-phase medium when there is a moving phase interface; the exact distribution is also dependent on the mixing occurring in the core of a casting. Concentration-induced convection is one of the main causes of mixing.

Here it is assumed that the temperature differences arising at $\tau \neq 0$ on reducing the temperature of the boundaries to the crystallization point are insufficient to produce thermal convection in the melt.

The solubility difference between the solid and liquid phases causes spatial nonuniformity in the impurity pattern. The liquid core of the solidifying melt therefore shows convection whose direction is dependent on the density relationship between the impurity and the parent melt. We have made a numerical study of the impurity distribution occurring under such conditions.

The melt has an initial temperature $T_0$ (reasonably close to the crystallization point) and fills a rectangular semiinfinite region in which the dimensions of the vertical cross section are $L_1 \times L_2$ at time $\tau = 0$; at that instant the melt is immobile and the impurity and temperature are uniformly distributed over the cross section.

The impurity distribution in the initial solution is taken as being 0.1-0.3%, so we take the phase-transition boundary as being isothermal, while the crystallization front migrates into the liquid region in accordance with a square-root law. It is assumed that the solidification occurs in all directions at the same rate:

$$\varepsilon_1 = l_1 - \alpha\sqrt{\mathrm{Fo}},\ \varepsilon_2 = l_2 - \alpha\sqrt{\mathrm{Fo}},\ R_1 = R_2 = \alpha\sqrt{\mathrm{Fo}}.$$

The transport of momentum and of the impurity is described for an incompressible liquid in general by a system of equations that includes the Navier—Stokes equation, the equation for mass transport, and the equation of continuity.

The characteristic velocity and the characteristic pressure difference are defined by

Donetsk State University. Translated from Inzhenerno-Fizicheskii Zhurnal, Vol. 34, No. 5, pp. 910-915, May, 1978. Original article submitted March 9, 1977.

 0022-0841/78/3405-0624$07.50 

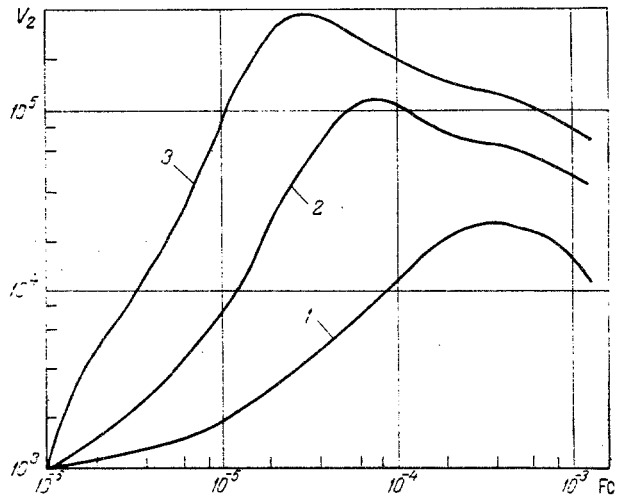


Fig. 1. Time course of the maximal vertical velocity: 1) $Gr_d = 0.2 \cdot 10^7$; 2) $0.2 \cdot 10^8$; 3) $0.2 \cdot 10^9$.

$$u_0 = \frac{\nu}{X_0}, \quad P_{\max} - P_{\min} = \rho u_0^2,$$

and then the differential equations are put in dimensionless form as follows:

1. the equation of motion

$$\frac{\partial \bar{V}}{\partial \mathrm{Fo}} + (\bar{V}\nabla)\bar{V} = -\nabla\pi + \mathrm{Sm}\,\nabla\bar{V} \pm \bar{l}_g\,\mathrm{Sm}^2\,\mathrm{Gr}_d S',$$

where S' is determined for each instant as the difference between the concentrations at the phase-transition boundary and at points lying on a net such that the concentration gradient beyond them may be neglected;

2. the mass-transport equation

$$\frac{\partial S}{\partial \mathrm{Fo}} + (\bar{V}\nabla)S = \Delta S;$$

3. the equation of continuity

$$\nabla\bar{V} = 0.$$

The boundary conditions, in addition, are

$$\bar{V}|_{\mathrm{Fo}=0} = 0, \quad S|_{\mathrm{Fo}=0} = 1$$

for $\eta_1 = R_1$, $\eta_1 = \varepsilon_1$, $\eta_2 = \varepsilon_2$, $\eta_2 = R_2$, $V_1 = V_2 = 0$.

The boundary conditions for the concentration are written for each boundary of the region, and the difference in solubility between the solid and liquid phases is incorporated via the equilibrium partition coefficient k, while diffusion in the solid state is neglected:

$$-\frac{\partial S}{\partial \eta_1}\Big|_{\eta_1=\varepsilon_1} = \varepsilon_1'(1-k)S|_{\eta_1=\varepsilon_1}, \quad -\frac{\partial S}{\partial \eta_1}\Big|_{\eta_1=R_1} = R_1'(1-k)S|_{\eta_1=R_1},$$

$$\frac{\partial S}{\partial \eta_2}\Big|_{\eta_2=R_2} = R_2'(1-k)S|_{\eta_2=R_2}, \quad -\frac{\partial S}{\partial \eta_2}\Big|_{\eta_2=\varepsilon_2} = \varepsilon_2'(1-k)S|_{\eta_2=\varepsilon_2}.$$

Finite-difference mthods are used with an integral interpolation method [1] or fractional-step methods [2], or else by introducing the stream function $\psi$ and the circulation velocity $\varphi$. We transfer to unit region $\zeta_1$, $\zeta_2$ with time-constant boundaries [3].

The $\mathrm{Sm}^2\mathrm{Gr}_d S$ term in (1) is taken as positive, which corresponds to the density of the parent melt being less than that of the impurity.

Numerical implementation by computer was based on a coordinate net $\omega_h$ and a time net $\mathrm{Fo}_n$: It was assumed that the numbers of intervals along each of the coordinates $\zeta_1$ and $\zeta_2$ are the same (I = M), which gives

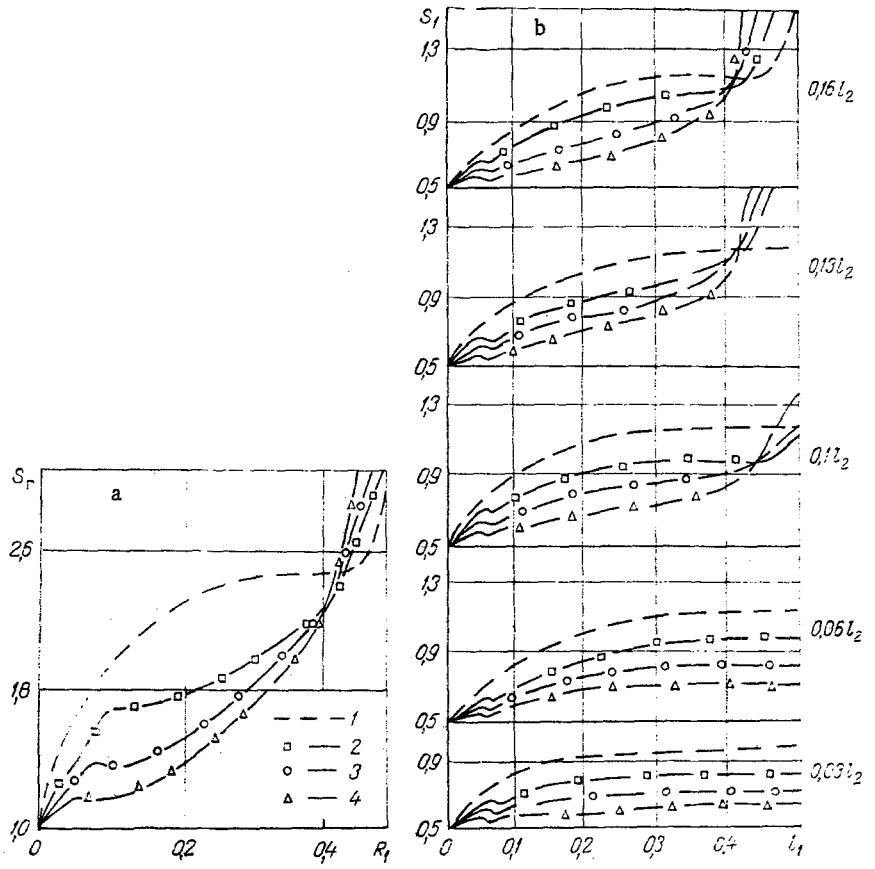


Fig. 2. a) Impurity distribution at the phase-transition boundary; b) impurity distribution in the solidified melt: 1) $Gr_d = 0$; 2) $0.2 \cdot 10^7$; 3) $0.2 \cdot 10^8$; 4) $0.2 \cdot 10^9$.

$$\omega_h = \left\{ \zeta_1 = ih,\ \zeta_2 = mh,\ h = \frac{1}{I} = \frac{1}{M} > 0, \right.$$

$$\left. i = 0,\ 1,\ 2,\ \ldots,\ I,\ m = 0,\ 1,\ 2,\ \ldots,\ M \right\},$$

$$\mathrm{Fo}_n = \left\{ \mathrm{Fo} = \sum_{j=0}^{n} \tau_j,\ \tau_j = A\frac{h^2}{4},\ 0 < A < 1 \right\}.$$

The difference scheme was implemented with a Dnepr-21 computer.

The net was taken as 32 × 32 on the basis of the available store of the machine and the conditions for mathematical stability.

The relative error of the calculation was determined as not more than 5%.

The following values were used for the parameters:

$$\mathrm{Sm} = 90,\ \alpha = 10,\ k = 0.5,\ x_0 = 0.6\ \mathrm{m},\ \mathrm{Gr_d} = 0.2 \cdot 10^n (n = 7,\ 8,\ 9).$$

The impurity is uniformly distributed over the liquid core at the start; the excess impurity is rejected by the solid at the phase boundary, because the equilibrium partition coefficient was taken as less than 1; this resulted in a concentration nonuniformity at the boundary, and the accumulating impurity caused the fluid to circulate, with the influx of fresh liquid less enriched in impurity. The result of this gravitational process is that two eddies arise in the liquid core, which provide convective mixing.

The convection rate increased substantially with $Gr_d$; in addition, there was a fall in the time needed to reach the maximum speed, which itself rose (Fig. 1). Also, the motion remained largely unchanged up to the end of solidification, which agrees well with many experiments [4]. The convection currents accelerate the transport of the impurity away from the phase-transition boundary and thus substantially influence the concentration pattern. The

latter alters considerably as soon as solidification starts, and high concentration gradients arise, which accelerate the convective motion. The concentration nonuniformity persists until the end of solidification, which is associated with rapid convection at all stages.

The impurity concentration is highest at the center because the flows enriched in the impurity descend to the bottom, while the rising flows from the center transport fresh material to the solidifying surface.

The details of the convection under these conditions were examined by calculating the impurity or dopant distribution in a melt at rest. Figure 2a compares the distributions arising near the phase boundary with and without convective motion and indicates that there is a substantial fall in the impurity concentration in the solid until about 70% of the melt has solidified, after which there is a sharp rise. This fall is clearly due to the accelerated impurity transport away from the boundary when convection occurs.

The sharp rise in impurity concentration at the end of the solidification is due to the highly enriched core and, in addition, to the rapid removal of the heat from the remaining small volume of liquid.

Figure 2b shows the impurity distributions arising with and without convective motion.

Concentration-induced convection produces a substantial enrichment in impurity at the center with depletion at the periphery, evidently on account of the distribution arising in the liquid core under conditions set up by the convection at the phase-transition boundary.

An increase in $Gr_d = 0.2 \cdot 10^n$ (n = 8 or 9), which is equivalent to increasing the speed of the convection, tends to accelerate and accentuate these effects.

The numerical calculations agree well with the conclusions drawn in [5].

## NOTATION

$L_1$, width of crystallizer cavity; $L_2$, height of cavity; $X_0$, characteristic dimension of region; $X_1$, horizontal coordinate; $X_2$, vertical coordinate; $\ell_1 = L_1/X_1$, relative width; $\ell_2 = L_2/X_2$, relative height of cavity; $\eta_i = X_i/X_0$ (i = 1, 2), dimensionless coordinate; $\varepsilon_i = Z_i/X_0$ (i = 1, 2), dimensionless width of liquid zone; $R_i = r_i/X_0$ (i = 1, 2), dimensionless thickness of solid crust; $\tau$, time; $Fo = D\tau/X_0^2$, dimensionless time; D, diffusion coefficient; $\bar{u}$, convective velocity; $\bar{V} = \bar{u}/u_0$, dimensionless convective velocity; $V_1$, $V_2$, dimensionless horizontal and vertical convective velocity components; $P_{max}$, $P_{min}$, total and hydraulic pressures; $\varepsilon_i' = d\varepsilon_i/dFo$, $R_i = dR_i/dFo$ (i = 1, 2), rates of variation in zone and crust thickness; K, equilibrium impurity partition coefficient; $C_0$, initial impurity concentration; C, impurity concentration in liquid; $C_1$, impurity concentration in solid; $S = C/C_0$, dimensionless impurity concentration in liquid; $S_1 = C_1/C_0$, dimensionless impurity concentration in solid phase; $S_b = C_b/C_0$, dimensionless concentration at phase interface; $\pi = P/(P_{max} - P_{min})$, dimensionless pressure; $Gr_d = \gamma g C_0 X^{03}/\nu^2$, diffusion Grashof number; $\gamma = 1/\rho \cdot \Delta\rho/\Delta C$; $\alpha$, solidification coefficient; $Sm = \nu/D$, Schmidt number; $\nu$, kinematic viscosity; $\rho$, density; $\zeta_1 = (\eta_1 - R_1)/(\varepsilon_1 - R_2)$ and $\zeta_2 = (\eta_2 - R_2)/(\varepsilon_2 - R_2)$, dimensionless coordinates for transition to unit time region; g, acceleration of gravity; h, step in coordinate net; $\tau_j$, step in time net; i, m, numbers of divisions for horizontal and vertical coordinates; $\bar{\ell}_g$, unit gravity vector.

## LITERATURE CITED


1. A. A. Samarskii, An Introduction to Difference Schemes [in Russian], Nauka, Moscow (1971).
2. N. N. Yanenko, A Fractional-Step Method of Handling Multiparameter Problems in Mathematical Physics [in Russian], Nauka, Novosibirsk (1968).
3. P. F. Zavgorodnii, I. L. Povkh, and G. M. Sevost'yanov, Zh. Prikl. Mekh. Tekh. Fiz., No. 2 (1975).
4. V. A. Efimov, in: Proceedings of the Second Conference on Casting: Physicochemical and Thermophysical Processes in the Crystallization of Steel Castings [in Russian], Metallurgiya, Moscow (1967).
5. É. A. Iodko, P. F. Zavgorodnii, F. V. Nedopekin, et al., Izv. Vyssh. Uchebn. Zaved., Chern. Metallurg., No. 5 (1972).